Active feedback control on post-mission disposal compliance to limit the space debris proliferation

Martina Rusconi[(1)], Camilla Colombo[(2)]

[(1)]*Politecnico di Milano*
Milan, Italy
martina.rusconi@polimi.it

[(2)] *Politecnico di Milano*
Milan, Italy
camilla.colombo@polimi.it

***Abstract* – Space utilisation faced unforeseeable changes in the last decades. However, the policy definition for debris mitigation has not matched the rapid growth of the inert population on orbit. The interdisciplinary framework proposed in the GREEN SPECIES project, funded by the European Research Council, aims at providing scientific support to the reactive definition of regulations and at systematic investigating debris mitigation strategies. In this respect, this paper focusses on the concurrent development of a propagator of the objects' dynamics with sources, sinks and mitigation measures and of a feedback controller acting on the population. The objects orbiting low-Earth space are modelled as a fluid with continuous properties. A deposition profile is modelled along with a term emulating post-mission disposal of objects. As a first approach, a feedback, proportional and linear control logic automatically selects the post-mission disposal compliance of the deposited objects, to limit the growth of the inert population on orbit. An example of the methodology is provided, and the results discussed in terms of validity of the approach.**

I. INTRODUCTION

The problem of an uncontrolled debris proliferation has been discussed since the '70s, when Kessler and Cour-Palais raised attention on the exponential generation of small particles in the next future [1]. Since then, the focus of the scientific community has been set on the definition of models to better understand the debris problem and to predict the evolution of the inert space population. As of today, many agencies and institutions developed their own debris propagator, such as the European Space Agency's (ESA) DELTA [2], the LEGEND model of the National Aeronautics and Space Administration (NASA) [3] or SDM of the Italian National Research Council [4]. Following simulation results, a first attempt to limit the debris proliferation was made with the Inter-Agency Debris Committee (IADC) formulation of mitigation guidelines in 2002, that provided requirements for mission design and operations to limit the probability of debris generation [5]. However, utilisation of the space environment faced unforeseeable changes in the last decades. Miniaturisation of technologies and more affordable access to space caused increased launch traffic, with private actors gaining a major role in the current space economy. These factors contribute to the dramatic growth of inert objects in-orbit, with consequent rise of the probability of collision with active satellites [6]. In this new scenario, a common outcome of the many years of research and despite the different modelling techniques, is that the current exploitation of the orbital environment is not sustainable, even with wider adoption of the IADC mitigation guidelines [6]. Consequently, it is necessary to revisit and update the guidelines and define policies for mission design that are up to date with the current space exploitation. ESA took the lead in this direction formulating a new set of internal requirements for sustainability compliance of its missions, following years of research and data [7]. However, the slowness in policy definition is an issue when facing the fast-evolving environment that became the space sector. Thinking back at the early 2000s, the number of objects launched nowadays would have been unpredictable and the same unpredictability applies to future activities.

Aim of the GREEN SPECIES project, funded by the European Research Council, is the development of an adaptive tool to support the prompt definition of guidelines to enforce a sustainable utilisation of space. As a starting point, similar complex systems are considered, such as climate change evolution and epidemics spread, which face quick and dramatic changes in their evolution, involve large spatial scales and require reactive policies [8][9][10]. Taking example from the techniques applied in those fields, the project proposes to automate as much as possible the process of analysis and definition of regulations by developing an interdisciplinary framework for modelling and control of the debris population. Core activity is the integration of a simulator for the evolution of the space objects' population with an active feedback controller on the environment, a schematic of which is provided in Fig. 1. Previous works in this direction for the debris problem can be found in literature [11][12], that dealt with automatic feedback definition of Active Debris Removal (ADR) annual rate based on simplified models of the debris population.

The project is in its development phase and, in the following work, the preliminary one-dimensional model of in-space objects' density propagation and its

integrated linear feedback controller are presented. In Section II the model and control blocks' current versions are described, in Section III a simple example of the method application is provided. Finally, in Section IV the main conclusions are summarised.

II. METHODOLOGY

In the GREEN SPECIES project three main building blocks are connected to create a new interdisciplinary framework for debris evolution and its control. As depicted in Fig. 1 a model of the space objects' population is developed along with an active controller of its evolution; the outcomes of these blocks will then be processed to support definition of policies and regulations for debris mitigation. The work described in the following focusses on the model and the control tasks, which are being developed concurrently to enforce correct integration of the two elements. At the end of the work a versatile controller will act on simplified models of the debris environment for fast and preliminary analyses, and on complex systems for more accurate results. Moreover, robustness will be enforced to deal with the unavoidable uncertainties of evolutionary models.
In this early development phase, a one-dimensional propagator of the population density is controlled with a proportional linear feedback logic.

A. The model

The model exploits a density-based formulation, in which the population of objects is described as a flow with continuous properties evolving in time and space. This approach has been extensively validated in literature, and its benefits in terms of computational cost and the method's accuracy have been analysed and documented. The first to propose the application of continuum mechanics to small non-interacting particles was Heard in the 70's [13]. Later, McInnes was the first to develop a fully analytical solution for debris density propagation in Low Earth Orbit (LEO), under the effect of atmospheric drag, considering some simplifying assumptions such as quasi-circular orbits for the objects [14]. Then, in [15] Letizia et al. developed the CiELO suite, exploiting the analytical method by McInnes for the propagation of in-orbit fragmentations. The problem

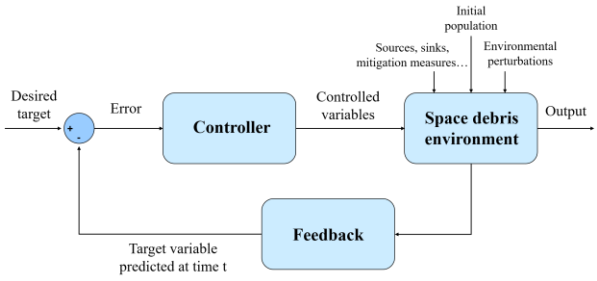

Fig. 1. Block scheme of the model-control system that is being developed within the GREEN SPECIES project.

was also extended to multiple dimensions and different force models, adding the J2 perturbation and solar radiation pressure to the drag effect [16]. The Starling suite developed by Frey et al. [17] put the basis for debris cloud propagation under any nonlinear dynamics and in multiple dimensions; then Giudici et al. carried on the work with a fully probabilistic model that numerically propagates the density of a continuous flow in all the orbital elements and physical properties of the objects, and in any dynamical regime [18].
The continuum approach was also applied to the propagation of the whole debris population by Colombo et al. [19] and extended to consider for feedback effect of fragmentations in Duran et al. [20]. A multi-dimensional model based on the continuity equation was then proposed by Giudici et al., and it is embedded in the COMETA tool, developed at Politecnico di Milano, for the future projection of the in-orbit population under the effect of objects' sources and sinks, and mitigation actions [18].
These models have the advantage of being agnostic to the number of fragments considered and the reduced dimensionality of the problem makes them suited to the application of an external control. As previously stated, even if multi-dimensional complex models for debris population's evolution are available at Politecnico di Milano [18], the preliminary phase of control development is built on a one-dimensional system in orbital radius. Leveraging on the work by McInnes and Letizia et al. [14][15], the spatial domain is binned in spherical shells, each delimited by an upper and a lower radius. The model exploits the conservation of the number of objects in time in terms of spatial density n. In every fixed volume V the integral form of the continuity equation (1) is propagated in time, where the term $(v_r n)$ accounts for the density flux flowing in and out the shell surfaces S with radial velocity v_r, and the terms $\dot{n}^+$ and $\dot{n}^-$ are source and sink density rates that directly add or remove objects in the considered volume.

$$\frac{dn}{dt} = \frac{1}{V}\left[-\int_S (v_r n) dS + \int_V \dot{n}^+ - \int_V \dot{n}^-\right] \qquad (1)$$

A graphical representation of the domain is given in Fig. 2. This approach is defined as the finite volume method [21]. The work in [22] was adapted to the one-dimensional case and the governing equation (1) obtained applying the divergence theorem to the differential form of the same, i.e. integrating over the spherical shell volume.
The natural dynamics term v_r comes from the rate of loss energy due to atmospheric drag [14], and is modelled as in (2). μ is the gravitational parameter of the Earth and R_E the Earth's radius, r is the orbital radius associated to the volume, which is taken as the value at the centre of the shell, $\frac{A}{m}$ is the average area to mass ratio of the objects whose density is propagated, C_D is the drag coefficient, typically considered equal to 2.1 from

flat plates assumption, ρ and H are the local air density and the reference scale height, respectively, which are modelled exploiting the superimposition of exponential functions described in [23].

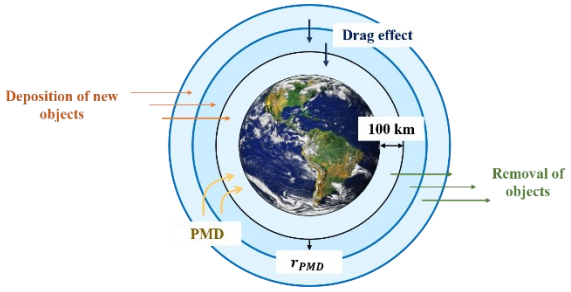

Fig. 2. Graphical representation of the space environment domain model. The arrows in and out of the shells represent deposition, removal, and motion of objects.

$$v_r = -\sqrt{\mu r}\frac{A}{m}C_D\rho \exp\left(-\frac{r-R_E}{H}\right) \quad (2)$$

The deposition and removal terms $\dot{n}^+$ and $\dot{n}^-$ include all the effects changing the rate of density that are not caused by the dynamical flow of the same. In the debris problem, these contributions may account for launches, ADR or Post-Mission Disposal (PMD) of objects. Equation (3) describes the currently modelled dynamics of the density, it applies to each i^{th} spherical shell delimited by lower and upper orbital radii values, $r_{i_{lower}}$ and $r_{i_{upper}}$, resulting in a system of ordinary differential equations. Since only one species of objects is accounted for in the preliminary model described, it is assumed that it represents only the intact objects population. The fast-evolving effects include a source term $f(r,t)$, that is defined as a continuous function in time and orbital radius for the deposition of new objects per unit time and unit radius, whose volume integral provides the density rate in that shell. It models launches of new intact objects in space, that contribute to the debris population, similar to what was done in [12]. The second contribution $g(r,t)$ accounts for removal and deposition of objects emulating a PMD profile in the domain. A percentage $\lambda_i \in [0,1]$ of the objects eligible for disposal in each higher altitude shell with $r_{i_{upper}} > r_{PMD}$ is removed and added to the first available volume completely below the compliance limit r_{PMD}. To set a value for r_{PMD}, a time for disposal t_{PMD} is assigned to the population. t_{PMD} identifies the time span in which the disposed objects are required to fall below the limiting re-entry radius due to drag, which is set at 200 km altitude. This translates into a requirement in the maximum orbital radius to be compliant, that is obtained solving the implicit relation proposed by King-Hele (4), where r_0 is the re-entry limit previously defined and equal to 200 km altitude, and r_{PMD} is the compliance limit, assuming circular orbits for the objects subject to drag effect only and assuming constant air density and scale height computed at r_{PMD}: $\rho_{r_{PMD}}$ and $H_{r_{PMD}}$ [24]. The $g(r,t)$ function, that identifies the objects per unit time and unit radius that reached end of life at the current time and might manoeuvre for re-entry, is defined as in (3). $\int_{r_{i_{lower}}(t_{dep})}^{r_{i_{upper}}(t_{dep})} f(r,t_{dep})$ is the number of objects added to the i^{th} control volume at time $t_{dep} = t - t_{life}$, where t is the current instant and t_{life} is the time the population of deposited objects spends orbiting under the drag effect before manoeuvring for end-of-life disposal. The control volume at time t_{dep} is identified by the orbital radii limiting the current shell backpropagated up to deposition time as $r_{i_{lower/upper}}(t_{dep}) = \int_t^{t_{dep}} -v_{r_{i_{lower/upper}}} dt$. In other words, assuming to follow a shell of the domain back in time, its shape changes from t to t_{dep} under drag effect. Considering that the deposited objects are assumed to have a residual orbiting life before manoeuvring for PMD, similarly to the approach in [12], the objects added to that same volume at t_{dep} are the ones reaching end-of-life at t in the control volume of the domain. Since only objects added through the source f are considered for disposal, the term g becomes active from time $t = t_0 + t_{life}$, with t_0 initial instant.

$$\frac{dn_i}{dt} = \frac{1}{V_i}\left[-\left(4\pi n_{i+1} v_{r_{i+1}} r_{i_{upper}}^2 - 4\pi n_i v_{r_i} r_{i_{lower}}^2\right) + \int_{r_{i_{lower}}}^{r_{i_{upper}}} f\,dr + g_i\right] \quad (3)$$

where:

j = shell with $r_{j_{lower}} \le r_{PMD} \le r_{j_{upper}}$

- $for\ i = 1, \dots, j-1$
  $g_i = 0$
- $i = j-1$:

$$g_i = \sum_{r_{i_{upper}} > r_{PMD}} \lambda_i \int_{r_{i_{lower}}(t_{dep})}^{r_{i_{upper}}(t_{dep})} f(r,t_{dep})$$

- $i = j, \dots, N$:

$$g_i = -\lambda_i \int_{r_{i_{lower}}(t_{dep})}^{r_{i_{upper}}(t_{dep})} f(r,t_{dep})$$

$$t_{PMD} = \frac{\left[1-\exp\left(-\frac{1}{H_{r_{PMD}}}(r_{PMD}-r_0)\right)\right] H_{r_{PMD}} \sqrt{\frac{r_{PMD}^3}{\mu}}}{\rho_{r_{PMD}} \frac{A}{m} C_D r_{PMD}^2} \quad (4)$$

In the preliminary model discussed, f and g are continuous functions in time and orbital radius. Different profiles of deposition and removal scenarios can be investigated, and their parameters controlled. This would allow analyses of different contributions and regulations for acting on the in-orbit objects population, both in time and space. The dynamics in (3) is a first step to a complete definition of the debris population environment. Collisions and explosions contributions

may be regarded to be part of the source term f as functions of time and radius only. However, fragmentation models based on the collision probability of the objects typically introduce nonlinearities in the dynamics [12][20] and will be accounted for in future work.

B. The controller

The literature on active control applied to the space debris problem is reduced. A first approach to the problem is found in [11], where the author developed an adaptive strategy for the definition of the annual number of ADR. Similarly to a model predictive approach, a simplified plant was used to investigate the outcomes of different ADR rates in the next future and to select the best strategy in terms of number of population objects. Then, Somma et al. [12] took on from the previous work and integrated a statistical model of the objects' population with a proportional feedback control to adequately tune the ADR rate based on the error of the overall population density with respect to a target one. Concerning similar applications, the active control of population growth has been widely applied to epidemics models, where feedback controls are exploited to investigate the effects of vaccination campaigns. In these works, susceptible and infected individuals interact through disease transmission rates and the system can be controlled by introducing vaccines [10] or biological control [9] of the population. It is a problem of proliferation containment, the more the number of infected patients, the more the epidemy spreads; similarly, the larger the number of debris, the more the collisions that generate fragments.

As clear from literature, a feedback approach is widely used due to its continuous adaptation to the current state of the plant, which makes it adequate to deal with a fast-evolving scenario. Moreover, a proportional law is typically the first choice to be investigated when defining a controller. Consequently, in this work a proportional linear feedback control is considered for the preliminary version of the plant.

From (3) λ is chosen as the input variable of the system, so the controller acts on the ratio of objects eligible for disposal that successfully manoeuvre to lower altitudes. The system of ordinary differential equations generated from (3) is reformulated in a linear time-variant state-space representation of the type (5), where the state $\boldsymbol{x}$ is the vector of the densities of the N shells, $\boldsymbol{u}$ is the control, and $\boldsymbol{x}_0$ is the given initial density profile. $\boldsymbol{F}(t)$ in (5) is the state matrix, which is constant and accounts for the drag dynamics. $\boldsymbol{G}(t)$ is the control matrix that maps the input variable to its effect on the state. In Section III $\boldsymbol{u}$ is treated both as a vector, meaning different compliance for each of the M shells with $r_{i_{upper}} > r_{PMD}$, for which $\boldsymbol{G}(t)$ takes the matrix shape in (5), and as a single value, meaning same compliance for all the higher shells, for which $\boldsymbol{G}(t)$ is adequately shaped in vector form of dimension Nx1. Finally, $\boldsymbol{C}(t)$ is the disturbance vector that includes all the sources that do not depend on the state, meaning the deposition term in (3).

$$\begin{gathered}\dot{\boldsymbol{x}} = \boldsymbol{F}(t)\boldsymbol{x}(t) + \boldsymbol{G}(t)\boldsymbol{u}(t) + \boldsymbol{C}(t), \\ \boldsymbol{x}_0 \text{ given}\end{gathered} \tag{5}$$

where:

$$\boldsymbol{F}_{NxN} = \begin{bmatrix} F_{1,1} & F_{1,2} & 0 & \dots & 0 \\ 0 & \ddots & \ddots & & \\ \vdots & & F_{i,i} & F_{i,i+1} & \\ & & & \ddots & \ddots \\ 0 & & & & F_{N,N} \end{bmatrix}$$

$$F_{i,i} = \frac{1}{V_i}\left(4\pi v_{r_i} r_{i_{lower}}^2\right)$$

$$F_{i,i+1} = \frac{1}{V_i}\left(-4\pi v_{r_{i+1}} r_{i_{upper}}^2\right)$$

$$\boldsymbol{G}_{NxM} = \begin{bmatrix} 0 & \dots & 0 \\ \vdots & \ddots & \vdots \\ G_j & G_{j+1} & \dots & G_M \\ -G_j & 0 & \dots & 0 \\ 0 & -G_{j+1} & 0 & \vdots \\ & 0 & \ddots & 0 \\ & \dots & 0 & -G_M \end{bmatrix}$$

$$G_j = \frac{1}{V_i} g_j \text{ for } j = \text{shell with } r_{i_{lower}} > r_{PMD}$$

$$\boldsymbol{C}_{Nx1} = \begin{bmatrix} C_1 \\ \vdots \\ C_i \\ \vdots \\ C_N \end{bmatrix}$$

$$C_i = \frac{1}{V_i}\int_{r_{i_{lower}}}^{r_{i_{upper}}} f dr$$

A linear feedback control law acts on the system (5) changing the λ value to reach a target density profile in orbital radius, in a fixed time span. The control problem deals with the minimisation of the cost function in (6), made up of a quadratic form in the terminal error of the state ($\boldsymbol{e}_f$) with respect to the target ($\boldsymbol{x}_d$) and an integral from initial to final times, t_0 and t_f, of quadratic terms of the control and state error variables. $\boldsymbol{A}$ and $\boldsymbol{B}$ are weight matrices defining acceptable levels of $\boldsymbol{e}$ and $\boldsymbol{u}$ in time, $\boldsymbol{S}_f$ is a weight matrix adding penalty on the final state.

$$J = \frac{1}{2}\boldsymbol{e}_f^T \boldsymbol{S}_f \boldsymbol{e}_f + \int_{t_0}^{t_f} \left(\frac{1}{2}\boldsymbol{e}^T \boldsymbol{A}\boldsymbol{e} + \frac{1}{2}\boldsymbol{u}^T \boldsymbol{B}\boldsymbol{u}\right) dt \quad \text{where } \boldsymbol{e} = \boldsymbol{x} - \boldsymbol{x}_d \tag{6}$$

The only constraints to the problem are provided by the dynamics (3) for all $t > t_0$. Applying the sweep method [25], the control law (7) is obtained. $\boldsymbol{S}$ is the time-dependant gain matrix computed backpropagating in time the differential Riccati equation, the vector $\boldsymbol{w}$ is added to the control to bring the state to a target different from zero and the vector $\boldsymbol{d}$ is required for disturbance rejection [26].

$$\boldsymbol{u}(t) = -\boldsymbol{B}^{-1}\boldsymbol{G}^T(\boldsymbol{S}\boldsymbol{x} + \boldsymbol{w} + \boldsymbol{d}) \tag{7}$$

For the system to be controllable it is required that the control action is capable of transferring any initial state to the final desired state within the given time span [27]. This has been checked with the matrix sequence method [28]. Indeed, being $\boldsymbol{F}$ and $\boldsymbol{G}$ $N-2$ and $N-1$ times differentiable, respectively, the matrix series (8) can be built and for the problem at hand it exists a time $t \in [t_o, t_f]$ for which (8) has rank equal to the state dimension, which is a sufficient condition for controllability, as stated by the theorems reported in [28].

$$\begin{aligned} \boldsymbol{M}_0(t) &= \boldsymbol{G}(t) \\ \boldsymbol{M}_k(t) &= -\boldsymbol{F}(t)\boldsymbol{M}_{k-1}(t) + \frac{d\boldsymbol{M}_{k-1}(t)}{dt} \\ &\text{for } k = 1, \dots, N-1 \end{aligned} \tag{8}$$

Finally, a saturation block is added after the controller to keep λ within its feasibility limits $[0, 1]$.
In Section III the presented approach is used on simple examples showing applicability of the same, its versatility and novelty, with little attention to the realism of the simulations. Both the model and the control block will undergo future updates and extensions adding realism to the results.

III. Preliminary Results

An application of the model-control system described in Section II is now shown. The example has no claims on realism but will validate the methodology and provide insights on its potential. A simple initial Gaussian density profile is considered, of the form (9) and shown in Fig. 4, similar to the one in [14], with a_0, b_0 and c_0 constants (see Table 1).

$$n_0(r) = a_0 \exp\left(-\left(\frac{r - r_{ref}}{b_0}\right)^{c_0}\right) \tag{9}$$

The initial state does not represent a real scenario, however in future applications the profile can be customized to the purpose and a sampled density condition, based on real objects distribution, can be obtained through binning or spatial density computation in each shell. A single homogeneous population is considered with an average value for the area to mass ratio, and its evolution is simulated for 1000 days. The domain spans from 200 km in altitude up to 1000 km (from r_{min} to r_{max} in Table 1) and it is divided in 8 spherical shells of width 100 km. The density value associated to the bin is computed at the central radius of each volume. The system of equations (3) describes the dynamics of the problem: the initial profile evolves under the effect of atmospheric drag, deposition source and PMD-like effect. To keep generality of the analysis a simple linear function in r and t is considered for the f term, of the form (10).

$$f(r, t) = r + t \tag{10}$$

Fig. 3 shows the evolution of the initial state spatial distribution at time snapshots recorded every 100 days, including only the deposition effect. As expected, the

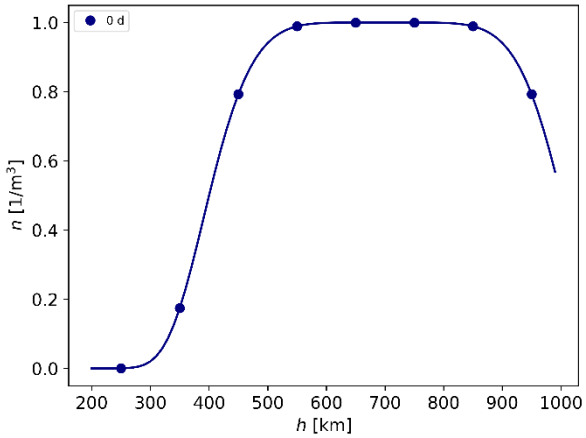

Fig. 4. Initial density profile in the altitude domain considered. The dots are the sampled values at the centre of each shell.

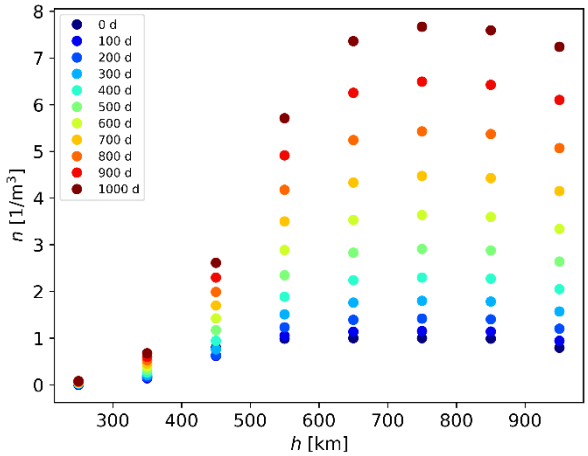

Fig. 3. Density values associated to the spherical shells of the domain captured every 100 days for 1000 days. The dynamics is affected by atmospheric drag and deposition of new objects.

density at high altitudes increases largely in time, both because the number of objects added to the environment grows linearly with r and t (10) and because the drag effect is much weaker than at lower shells. The same source profile enters in the definition of the PMD-like term in (3).

In Table 1 are listed the other model inputs required: the simulation time is set at 1000 days, t_{life} at 100 days, the t_{PMD} limit at 100 days, which translates in a compliance radius limit of about 400 km altitude.

Table 1. List of inputs to the analyses of Section III.

Simulation time	
t_0	$0\ s$
t_f	$86400000\ s$
Initial state inputs	
a_0	$1\ m^{-3}$
b_0	$7071\ km$
c_0	$318.9\ km$
k_0	6
Domain definition inputs	
$r_{min} = r_0$	$6571\ km$
r_{max}	$7371\ km$
Δr	$100\ km$
Drag inputs	
C_D	2.1
$\frac{A}{m}$	$0.0238 \frac{m^2}{kg}$
PMD inputs	
t_{life}	$100\ days$
t_{PMD}	$100\ days$
Control inputs	
$\boldsymbol{A}$	$\begin{bmatrix} \epsilon & 0 & \cdots & 0 \\ 0 & \epsilon & & \vdots \\ \vdots & & \frac{1}{a} & \\ & & & \ddots \\ 0 & \cdots & & \frac{1}{a} \end{bmatrix}$ $\epsilon = 10^{-15}\ s^{-1}m^6$ $a = t_f e_{max}^2$ $e_{max} = 1\ m^{-3}$
$\boldsymbol{S_f}$	$\begin{bmatrix} \epsilon & 0 & \cdots & 0 \\ 0 & \epsilon & & \vdots \\ \vdots & & \frac{1}{s} & \\ & & & \ddots \\ 0 & \cdots & & \frac{1}{s} \end{bmatrix}$
	$\epsilon = 10^{-15}\ s^{-1}m^6$ $s = {e_f}^2_{max}$ ${e_f}_{max} = 0.5\ m^{-3}$

Case 1		*Case 2*	
$\boldsymbol{u}$ shape	$M \times 1$	$\boldsymbol{u}$ shape	1×1
$\boldsymbol{G}$ shape	$N \times M$	$\boldsymbol{G}$ shape	$N \times 1$
$\boldsymbol{B}$	$\begin{bmatrix} \frac{1}{b} & 0 & \cdots & 0 \\ 0 & \ddots & & \vdots \\ \vdots & & & \\ 0 & \cdots & & \frac{1}{b} \end{bmatrix}$ $b = t_f u_{max}^2$ $u_{max} = 1$	$\boldsymbol{B}$	$\begin{bmatrix} \frac{1}{b} \end{bmatrix}$ $b = t_f u_{max}^2$ $u_{max} = 1$

The behaviour in Fig. 3 brought to the control parameters definition in Table 1. Indeed, the desired final state after 1000 days is set equal to a uniform profile in space of 2 m^{-3}, to limit the density growth due to f. The weight matrices $\boldsymbol{A}$, $\boldsymbol{B}$, and $\boldsymbol{S_f}$ have been set constant in time and such as to enforce a maximum control equal to 1, a maximum acceptable error value on the evolving state equal to 1 m^{-3} and a maximum acceptable error on the final state equal to 0.5 m^{-3}. The feedback control will continuously adapt the λ term in the volumes above the compliance radius limit in (5) to reach the target profile. Consequently, the weight matrices are defined so that the upper shells only are brought to the target. First, the control history in time is obtained applying the sweep method from [25], then its saturated effect is added to the evolution of the density profile.

As clear from Table 1, two cases have been considered. First, λ is varied independently in each shell, $\boldsymbol{u}$ is a vector and $\boldsymbol{G}$ is in its matrix form (5). Then, u is one single λ value equal in all the controlled volumes and $\boldsymbol{G}$ is a vector. In Fig. 6 the controlled density profile in space is provided at time snapshots every 100 days, and the saturated control profile is in Fig. 5. The objects are removed from the upper shells and moved to the first available volume compliant with PMD requirements. As desired, the densities of the shells above 400 km in Fig. 6 settle around the target value of 2 m^{-3}. At the beginning of the simulation the percentage of moved objects is closer to zero, allowing the density to get larger; with time the profile gets closer to the target and the number of removed objects must increase to face the growing deposition rate. However, in the final 200 days the saturated control above 500 km cannot face the source term and the density profile rises inevitably. The required removal rate is also diversified in space and λ is larger with increasing altitudes. This is due to two effects: the f deposition profile linearly grows with

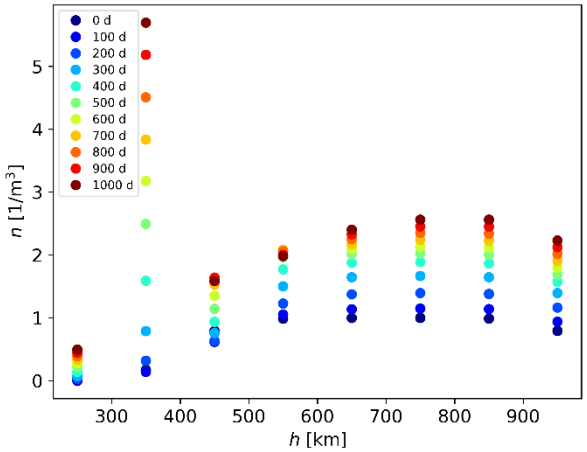

Fig. 6. Case 1 - Density profile evolution in space recorded every 100 days for 1000 days. Each dot represents the density associated to one shell. The dynamics is affected by atmospheric drag, deposition of new objects and the PMD-like term with λ controlled independently in each shell.

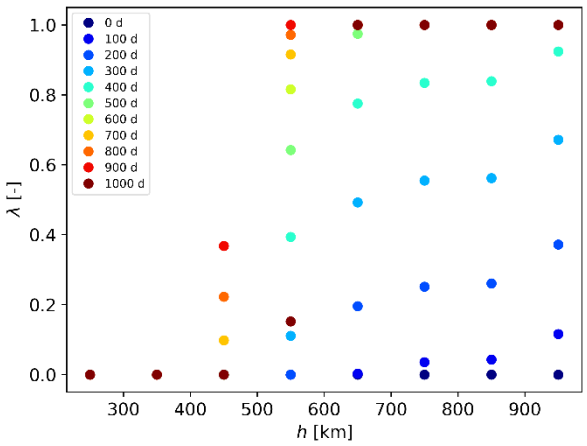

Fig. 5. Case 1 - Control input evolution in space recorded every 100 days for 1000 days. Each dot represents the λ associated to one shell. The control input is active only from the shell at 450 km on.

orbital radius requiring more objects removals in the uppermost shells to reach the same target density than the lower ones; indeed, the drag effect weakens with altitude causing accumulation of objects with rising radius, while in the lower shells a smaller percentage of removals combined with a stronger drag is enough to face the deposition of new objects and reach the target.

In Fig. 7 and Fig. 8 the density profile and control input evolution resulting from Case 2 are provided. The control variable is reduced to one single value and at every instant the same percentage of objects is removed from all the shells above 400 km. considering time steps of 100 days, λ is null for the initial 200 days, since the target density is larger than the initial condition in all the controlled shells. Then the removal action increases and, until 400 days have passed, the required λ is larger than

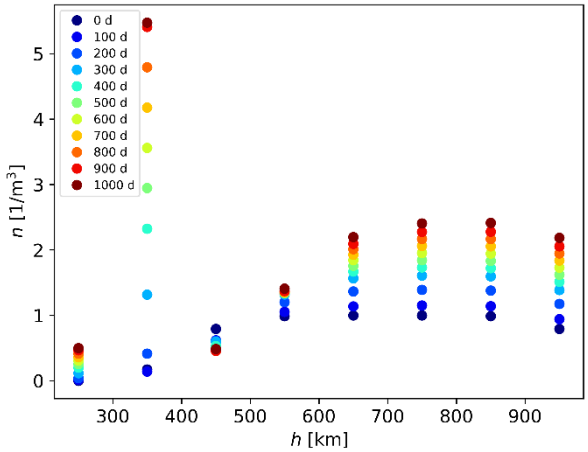

Fig. 7. Case 2 - Density profile evolution in space recorded every 100 days for 1000 days. Each dot represents the density associated to one shell. The dynamics is affected by atmospheric drag, deposition of new objects and the PMD-like term with one controlled λ value equal for all the shells from 450 km on.

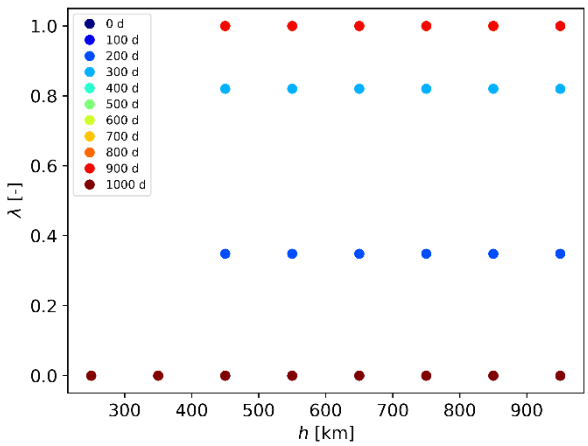

Fig. 8. Case 2 - Control input evolution in space recorded every 100 days for 1000 days. Each dot represents the λ associated to one shell (equal for all the controlled shells). The control input is active only from the shell at 450 km on.

the corresponding ones in Case 1 (see Fig. 8) in all the domain. From 500 days on the control is completely saturated everywhere to face the growing density at the highest altitudes, while in Case 1 the control below 700 km does not saturate for longer.

A. Discussion

The resulting density profile is similar in the two analysed cases. However, the condition of same removal percentage in all the high-altitude domain over-estimates the number of objects to move to reach the target. As clear from Fig. 5, the λ required in the uppermost shells is larger than the one in the lower domain, due to the accumulation effect caused by weak drag combined with a deposition rate linearly increasing

with orbital radius. For the same reasons this contribution influences largely the cost (6) and the control definition. Consequently, in Case 2 more objects are removed than necessary and deposited in the compliant volume and the saturation limit is enforced from 400 days on, while in Case 1 saturation is required in the upper domain after 500 days. This effect is also visible between 400 km and 600 km altitude in Case 2, where the final profile is lower than Case 1 and also lower than the targeted value. Similarly, at final time the density of the high-altitude shells in Fig. 7 is within the acceptable error, while in the lowest ones it is not, so the required λ settles at zero in all the domain to try and compensate for the missing objects below 600 km.

The simple example of this Section shows the capability of the feedback control to automatically tune the percentage of removed objects in time and space to reach a target. Provided a set of inputs and a final scenario, the controller selects the most suited inputs to fulfil the requirements. As shown, the proposed approach enables fast and critical comparison of different strategies. In fact, even if applied to unrealistic scenarios, the benefits of two different compliance profiles, aiming at the same final state, have been observed and quantified.

Different controls and final targets can be analysed exploiting the versatility of the approach. These preliminary results put the basis to future extensions and complexity addition in both model and control blocks.

IV. Conclusions

A model for in-space objects propagation and a feedback controller for population containment are concurrently under development within the GREEN SPECIES project. The preliminary versions of the two blocks have been presented. A simplified one-dimensional density-based model is exploited for the propagation of the population as function of the orbital radius. The density term evolves under the effect of drag dynamics and is affected by a source term and a PMD-like effect. A linear feedback control is applied to the linear time-varying system, and it actively tunes the percentage of objects to remove from the high-altitude shells to reach a target density profile. An example of the approach has been provided that showed the capability of the controller to define a suitable strategy in time to reach the desired final state. Moreover, critical comparison of two alternative mitigation procedures has been carried out, providing evidence of the versatility of the method.

Both the model and the controller will undergo extensions and updates in future work: fragmentations and multiple species will be added to the debris population definition and more advanced control logics will be investigated. Moreover, the potential of the method will be analysed considering different control inputs and target scenarios.

Aim of the project is to build an adaptive tool to systematically investigate different strategies for debris containment. The tool will be valuable in promptly reacting to the fast-evolving space situation and in providing scientific support to the definition of mitigation policies.

V. Acknowledgement

The research received funding from the European Research Council (ERC) under the European Union's Horizon Europe research and innovation program as part of the GREEN SPECIES project (Grant agreement No 101089265) and was partially supported by the ICSC—Centro Nazionale di Ricerca in High Performance Computing, Big Data, and Quantum Computing funded by European Union—NextGenerationEU.

VI. References

[1] D. Kessler, N. Johnson, J.-C. Liou, M. Matney. "The Kessler Syndrome: Implications to Future Space operations". *Advances in the Astronautical Sciences*. Vol. 137, 2010.

[2] B. Bastida Virgili. "Delta debris environment long-term analysis". *In Proceedings of the 6th International Conference on Astrodynamics Tools and Techniques (ICATT)*, 2016.

[3] J. C. Liou. "Legend – a three-dimensional leo-to-geo debris evolutionary model". *Advances in Space Research*, 34:981–986,1 2004.

[4] A. Rossi, L. Anselmo, C. Pardini, R. Jehn, and G. Valsecchi. "The new space debris mitigation (sdm 4.0) long term evolution code". *In Proceedings of the 5th European Conference on Space Debris*, 2009.

[5] Inter-Agency Debris Committee. "IADC Space Debris Mitigation Guidelines" Issued by IADC Steering Group and Working Group 4, 2021.

[6] ESA Space Debris Office. "ESA' s Annual Space Environment Report". *Technical report*, 2023.

[7] ESA Space Debris Mitigation Working Group. "ESA Space Debris Mitigation Requirements", *Issue 1*, 2023.

[8] M. Atolia, P. Loungani, H. Maurer, W. Semmler. "Optimal control of a global model of climate change with adaptation and mitigation". *Mathematical Control and Related Fields*, 2023, 13(2): 583-604. doi: 10.3934/mcrf.2022009.

[9] H.-L. Li, L. Zhang, Z. Teng, Y.-L. Jiang, A. Muhammadhaji. "Global stability of an SI epidemic model with feedback controls in a patchy environment". *Applied Mathematics and Computation*, Vol. 321, pp. 372-384, 2018. https://doi.org/10.1016/j.amc.2017.10.057.

[10] Y. Shang. "Global stability of disease-free equilibria in a two-group SI model with feedback control". *Nonlinear Analysis: Modelling and Control*. Vol. 20 pp. 501-508, 2015. doi: 10.15388/NA.2015.4.3.

[11] A. E. White, H. Lewis. “An adaptive strategy for active debris removal”. *Advances in Space Research*. Vol. 53, pp.1195-1206, 2014.
[12] G. L. Somma, C. Colombo, H. Lewis. “A Statistical LEO Model to Investigate Adaptable Debris Control Strategies”. *In Proceedings: 7th European Conference on Space Debris*. 2017.
[13] W.B Heard. “Dispersion of ensembles of non-interacting particles”. *Astrophys Space Sci*. Vol. 43, pp. 63–82, 1976. https://doi.org/10.1007/BF00640556.
[14] C. R. McInnes. “Simple analytic model of the long term evolution of nanosatellite constellations”. *Journal of Guidance Control and Dynamics*, 23(2):332–338, 2000.
[15] F. Letizia, C. Colombo, H. G. Lewis. “Analytical Model for the Propagation of Small-Debris-Object Clouds After Fragmentations”. *Journal of Guidance, Control, and Dynamics*. Vol. 38:8, pp. 1478-1491, 2015.
[16] F. Letizia. “Extension of the Density Approach for Debris Cloud Propagation”. *Journal of Guidance, Control, and Dynamics*. Vol. 41:12, pp. 2651-2657, 2018.
[17] S. Frey, C. Colombo, S. Lemmens. “Application of density-based propagation to fragment clouds using the Starling suite”. *In proceedings: First International Orbital Debris Conference*. 2019.
[18] L. Giudici, C. Colombo, A. Horstmann, F. Letizia, Francesca, S. Lemmens. “Density-based evolutionary model of the space debris environment in low-Earth orbit”. *Acta Astronautica*. Vol.219, 2024. 10.1016/j.actaastro.2024.03.008.
[19] C. Colombo, F. Letizia, H. Lewis. “Spatial density approach for modelling of the space debris population”. *In proceedings: 26th AAS/AIAA Space Flight Mechanics Meeting*. 2016.
[20] C. Duran, L. Giudici, C. Colombo. “Modelling the whole space debris environment through a spatial density approach”. *In proceedings: AAS/AIAA Astrodynamics Specialist Conference*. 2021.
[21] R.J. Leveque. “Finite-Volume Methods for Hyperbolic Problems”. *Cambridge University Press*, Cambridge, 2002.
[22] L. Giudici, C. Colombo. “Space debris density propagation through a finite volume method”. *In proceedings: 33rd AAS/AIAA Space Flight Mechanics Meeting*. 2023.
[23] S. Frey, C. Colombo, S. Lemmens. “Extension of the King-Hele orbit contraction method for accurate, semi-analytical propagation of non-circular orbits”. *Advances in Space Research*. Vol. 64, Issue 1, pp. 1-17, 2019. ISSN 0273-1177. https://doi.org/10.1016/j.asr.2019.03.016.
[24] D. King-Hele. “Theory of Satellite Orbits In an Atmosphere”. *Butterworths Mathematical Texts*. 1964. https://doi.org/10.1002/qj.49709038627.
[25] A.E Bryson. “Applied Optimal Control: Optimization, Estimation and Control”. *Routledge*, 1st ed., 1975. https://doi.org/10.1201/9781315137667.
[26] B. Gao, J. Hong, S. Yu and H. Chen. "Linear-quadratic output regulator with disturbance rejection: Application to vehicle launch control". *In proceedings: American Control Conference (ACC)*. pp. 1960-1965, 2017. doi: 10.23919/ACC.2017.7963239.
[27] R. Kalman. “Contribution to the Theory of Optimal Control”. *Boletin de la Sociedad Matematica Mexicana* ”. Vol. 5, 1960, pp. 102–119.
[28] Y. Wang, S. Liu, Q. Huang. “Controllability Analysis of Linear Time-Varying T-H Equation with Matrix Sequence Method”. *International Journal of Aerospace Engineering*. 2023.